

BEAM-DELIVERY CHALLENGES FOR PLASMA-WAKEFIELD ACCELERATORS

L. Kennedy^{*1,2}, C. Caliari², R. Tomás², R. D'Arcy¹, P. N. Burrows¹

¹John Adams Institute, University of Oxford, Oxford, United Kingdom

²European Organization for Nuclear Research, Meyrin, Switzerland

Abstract

Plasma-wakefield acceleration offers a promising path towards a next-generation collider, but poses significant beam-delivery challenges. We present initial designs for final-focusing systems capable of transporting beams from the plasma-based-collider concepts, ALiVE and HALHF, each with distinct beam dynamics constraints. For ALiVE, where the beams are intrinsically round, we demonstrate an increase in $\mathcal{L}_{1\%}/\mathcal{L}_{tot}$ from 3.6% to 27%, and explore ultra-compact FFS configurations reflecting the potential for significantly reduced collider lengths. For HALHF, where the beams feature large horizontal emittance to alleviate the burden on the plasma linac, we show that a global chromaticity-correction scheme reduces aberrations to within 20% of the design beam size at 375 GeV, and identify synchrotron radiation as the dominant limitation at higher energies.

INTRODUCTION

ALiVE [1] aims to deliver low-emittance beams using a highly relativistic, short proton driver to generate wakefields in the strongly nonlinear blowout regime. The beams generated in this scheme, with parameters given in Table 1, feature an intrinsically round transverse profile, leading to enhanced disruption and relatively few collisions occurring within 1% of the nominal energy due to strong beamstrahlung radiation. HALHF [2] proposes an electron-driven plasma-wakefield arm for electron acceleration and an RF linac for positron acceleration, bypassing the inherent difficulties associated with plasma-based positron acceleration. The beams generated in this regime are flat, with the horizontal emittance much greater than the vertical, with parameters given in Table 1 [3], and are therefore not dominated by beamstrahlung effects. However, the HALHF beams exhibit a large emittance, leading to considerable beam size growth due to transport aberrations in the CLIC final focus system (FFS) [4, 5]. FFS configurations based on the CLIC and traditional FFS schemes [6] are presented, addressing the challenges associated with plasma-based acceleration.

ALiVE FINAL FOCUS SYSTEM

ALiVE beams were tracked in a CLIC FFS using PLACET, with the resulting beam distributions used to compute the luminosity using GUINEA-PIG [7–9]. Total and peak luminosities of $\mathcal{L}_{tot} = 14.1 \times 10^{34} \text{ cm}^{-2}\text{s}^{-1}$ and $\mathcal{L}_{1\%} = 0.37 \times 10^{34} \text{ cm}^{-2}\text{s}^{-1}$ were found, corresponding to a relative fraction of the luminosity within the 1% energy

* lewis.kennedy@cern.ch

Table 1: Plasma Wakefield Beam Parameters For The Proton-Driven ALiVE And Electron-Driven HALHF Designs

Parameter	ALiVE	HALHF
Centre-of-mass energy [GeV]	250	250
Particles per bunch [$\times 10^{10}$]	2	1
e^- bunch length [μm]	105	150
e^+ bunch length [μm]	75	150
β_x^* at IP [mm]	13	3.3
β_y^* at IP [mm]	0.41	0.1
Norm. horizontal e^- emittance [nm]	100	90 000
Norm. vertical e^- emittance [nm]	100	320
Norm. horizontal e^+ emittance [nm]	400	10 000
Norm. vertical e^+ emittance [nm]	400	35
Bunch frequency [kHz]	7.2	16
Energy spread RMS [%]	0.10	0.15
Total luminosity [$10^{34} \text{ cm}^{-2}\text{s}^{-1}$]	9.3	1.2
Luminosity in top 1% [$10^{34} \text{ cm}^{-2}\text{s}^{-1}$]	0.34	0.76

peak of $\mathcal{L}_{1\%}/\mathcal{L}_{tot} = 2.5\%$ due to beamstrahlung effects. For a typical collider, an $\mathcal{L}_{1\%}/\mathcal{L}_{tot}$ greater than 30% should be expected in order to minimize background radiation and maximize the signal-to-noise ratio at the detector. It is therefore necessary to flatten the round ALiVE beam via the optical beta functions β_x^* and β_y^* in the FFS to maximize the $\mathcal{L}_{1\%}/\mathcal{L}_{tot}$ ratio.

The beta functions of a CLIC FFS were scanned by matching the FFS quadrupole strengths using MADX [10]. Figure 1 shows the total and peak luminosities as functions of β_x^* and β_y^* , demonstrating a linear reduction in beamstrahlung radiation due to beam flattening. A peak luminosity of $0.42 \times 10^{34} \text{ cm}^{-2}\text{s}^{-1}$ is found when $\beta_x^*/\beta_y^* = 80/0.11 \text{ mm}$, corresponding to 27% of collisions within 1% of the nominal energy. However, the total luminosity is degraded due to large β_x^* , enhanced synchrotron radiation from the Oide effect, and vertical aberrations induced by β_y^* squeezing [11]. Figure 2 shows the layout and linear optics of the FFS, with length $L_{FFS} = 550 \text{ m}$ and final drift length $L^* = 6 \text{ m}$.

Higher-order beam sizes were calculated semi-analytically using MAPCLASS [12–14], and were subsequently minimized using the higher-order multipoles in the FFS to reduce aberrations. Figure 3 shows good performance for the electron beam with RMS beam sizes of $\sigma_{x,e^-}/\sigma_{y,e^-} = 183/10 \text{ nm}$ at the interaction point (IP). However, due to a factor 4 larger positron emittance, the aberrations lead to enhanced beam size growth resulting in positron RMS beam sizes of $\sigma_{x,e^+}/\sigma_{y,e^+} = 428/71 \text{ nm}$ at the IP.

Exploratory studies assessed the performance of ultra-low β^* , ultra-short final focus systems for ALiVE, consistent

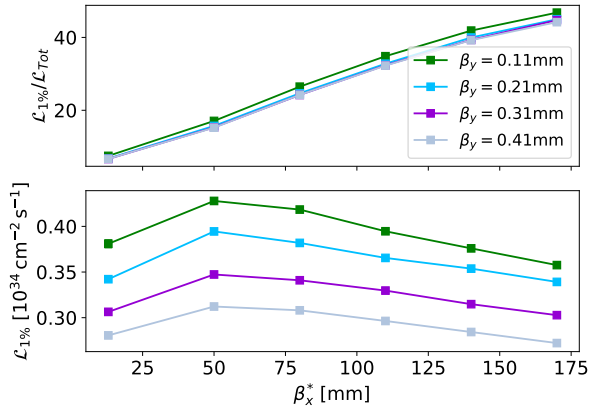


Figure 1: Relative fraction of the luminosity in the 1% energy peak (top) and absolute luminosity in the 1% energy peak (bottom), as functions of the optical beta functions β_x and β_y at the interaction point.

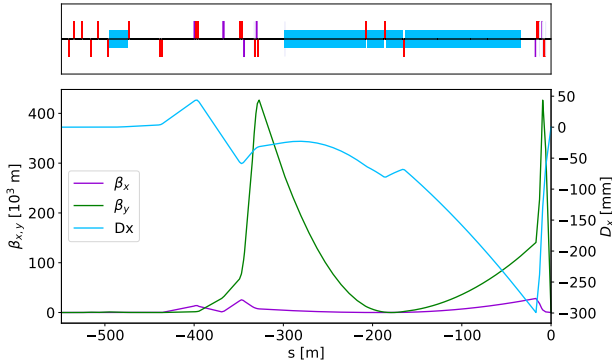


Figure 2: 550 m FFS linear optics (bottom) with lattice survey (top) including quadrupoles (red), dipoles (blue), sextupoles (purple), octupoles and decapoles (light purple). The IP is located at $s=0$ m.

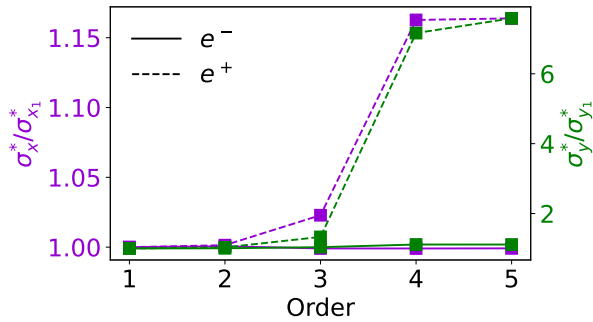


Figure 3: Aberrations up to the fifth-order, normalised to the first-order beam size, computed semi-analytically using MAPCLASS for the ALiVE electron and positron beams.

with the compact design objectives of plasma wakefield acceleration, but neglecting current magnet design limitations. Figure 4 shows the linear optics for an ultra-low β_y^* system with $L_{FFS} = 64$ m, $L^* = 0.5$ m, and $\beta_x^*/\beta_y^* = 60/0.02$ mm, delivering total and peak luminosities of $0.85 \times 10^{34} \text{ cm}^{-2} \text{ s}^{-1}$

and $0.37 \times 10^{34} \text{ cm}^{-2} \text{ s}^{-1}$, respectively. With $\mathcal{L}_{1\%}/\mathcal{L}_{tot}$ of 44%, this system offers the best signal-to-noise ratio, but does so with considerably lower absolute luminosities.

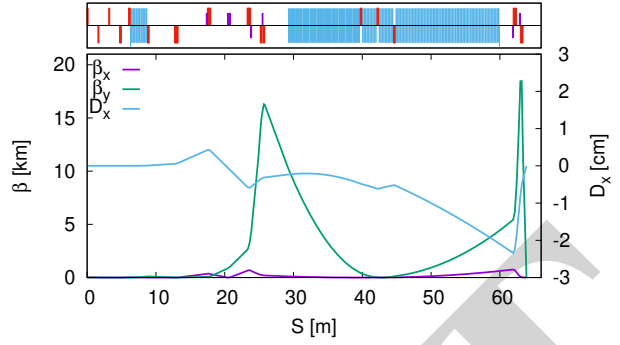


Figure 4: 64 m FFS linear optics (bottom) with lattice survey (top) including quadrupoles (red), dipoles (blue), sextupoles (purple), octupoles and decapoles (light purple). The IP is located at $s=64$ m.

An alternative configuration in which β_x^* is further squeezed was also explored, where $L_{FFS} = 45$ m, $L^* = 0.35$ m, and $\beta_x^*/\beta_y^* = 1.6/0.03$ mm, yielding total and peak luminosities of $14 \times 10^{34} \text{ cm}^{-2} \text{ s}^{-1}$ and $0.32 \times 10^{34} \text{ cm}^{-2} \text{ s}^{-1}$, respectively. While this system features an $\mathcal{L}_{1\%}/\mathcal{L}_{tot}$ of only 2%, it offers an ultra-compact FFS with performance on the level of the ALiVE design targets. A comparison between all of the ALiVE designs is presented in Table 2.

Table 2: Exploratory FFS Designs For The ALiVE Project

Parameter	ALiVE ¹	ALiVE ²	ALiVE ³
L_{FFS} [m]	550	45	64
L^* [m]	6	0.35	0.5
β_x^*/β_y^* [mm]	80 / 0.11	1.6 / 0.03	60 / 0.02
$e^- \sigma_{x/y}$ at IP [nm]	183 / 10	26 / 4	187 / 3
$e^+ \sigma_{x/y}$ at IP [nm]	428 / 71	68 / 13	345 / 8
\mathcal{L}_{tot} [$10^{34} \text{ cm}^{-2} \text{ s}^{-1}$]	1.6	14	0.85
$\mathcal{L}_{1\%}$ [$10^{34} \text{ cm}^{-2} \text{ s}^{-1}$]	0.43	0.32	0.37
$\mathcal{L}_{1\%}/\mathcal{L}_{tot}$ [%]	27	2.3	44
$\Delta p/p$ [%]	0.17	0.17	0.17

HALHF

Evaluation of higher-order beam sizes using the CLIC FFS with HALHF emittances shows substantial beam-size growth from geometric aberrations. Mitigation required replacing the compact CLIC FFS with a traditional chromaticity correction scheme. The resulting linear optics for an e^- beam with energy of 375 GeV, $L_{FFS} = 1500$ m, and $L^* = 2.2$ m, are shown in Fig. 5, with $\beta_x^*/\beta_y^* = 8.8/0.09$ mm.

Achieving beam sizes near HALHF targets requires reducing the emittances to $0.33\epsilon_x$ and $0.7\epsilon_y$. Aberrations were minimized up to the fifth order, yielding beam sizes within 20% of the design for the reduced-emittance beam as shown in Fig. 6. Synchrotron radiation from the Oide effect was mitigated by increasing the QF1 length to 8.8 m with proportionally reduced strength, while QD0 remains at 5.3 m.

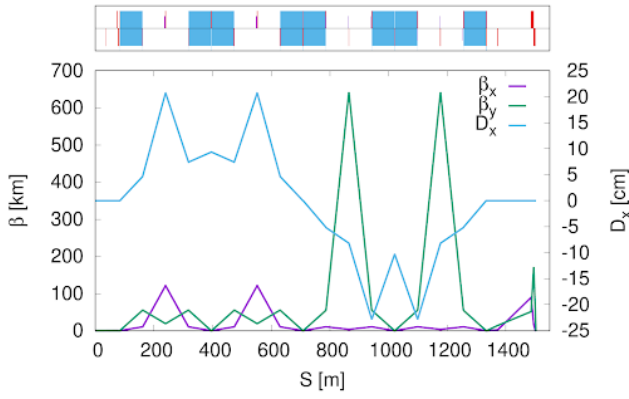


Figure 5: Traditional FFS used for HALHF. Linear optics (bottom) with lattice survey (top) including quadrupoles (red), dipoles (blue) and sextupoles (purple) are shown.

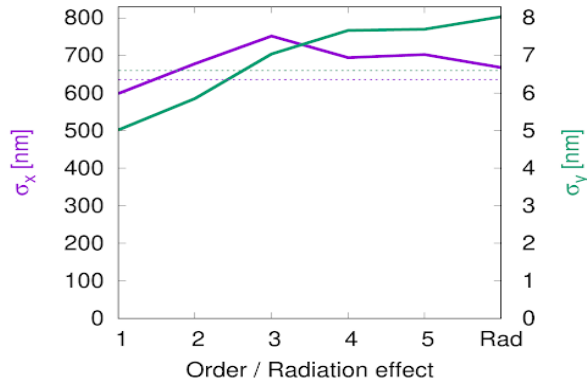


Figure 6: Semi-analytic evaluation of higher-order beam size effects using MAPCLASS, including aberrations up to the 5th order and synchrotron-radiation-induced growth for the 375 GeV electron beam with optimised QF1.

The resulting RMS beam size contribution is adequately suppressed as shown in Fig. 6. However, the performance of this system is significantly reduced with increasing beam energy due to synchrotron radiation from the FFS dipoles, as shown in Fig. 7. Improvements to the traditional FFS design and other compact FFS designs should be explored to reduce the FFS length and improve beam sizes at higher energies.

CONCLUSION

We have presented final-focusing-system designs for plasma-based colliders, addressing the beam-delivery challenges of ALiVE and HALHF. For ALiVE, round beams induce beamstrahlung radiation, reducing the fraction of luminosity within the 1% energy peak. These effects were mitigated by beam flattening via the optical beta functions β_x^* and β_y^* . A local chromaticity correction FFS based on the CLIC design, with a length of 550 m, $L^* = 6$ m, and $\beta_x^*/\beta_y^* = 80/0.11$ mm, yields total and peak luminosities of $1.56 \times 10^{34} \text{ cm}^{-2}\text{s}^{-1}$ and $0.42 \times 10^{34} \text{ cm}^{-2}\text{s}^{-1}$, respectively. In this configuration, 27% of collisions occur within 1% of the design energy, compared to 3.6% in the ALiVE proposal.

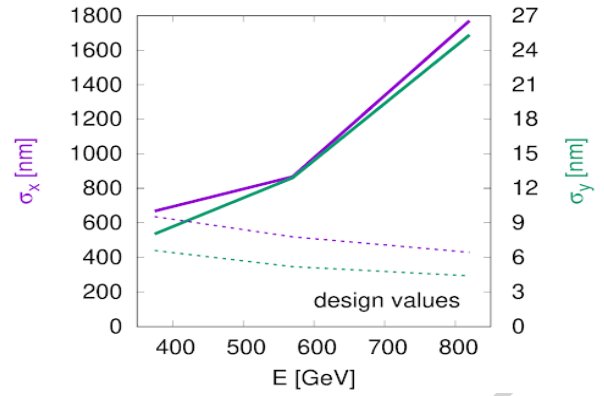


Figure 7: Optimized RMS beam sizes as a function of the electron beam energy with HALHF design parameters.

Ultra-compact alternatives were investigated, with one design prioritizing the fraction of luminosity within the 1% peak, achieving $\mathcal{L}_{1\%}/\mathcal{L}_{tot} = 44\%$ with an FFS length of 65 m and $L^* = 0.5$ m. A second configuration prioritizes total luminosity and compactness, reaching $14 \times 10^{34} \text{ cm}^{-2}\text{s}^{-1}$ with an FFS length of 45 m and $L^* = 0.35$ m.

For HALHF, a traditional chromaticity-correction FFS scheme reduced aberrations, achieving beam sizes within 20% of the design values at 375 GeV. However, this required reductions of 70% in the horizontal emittance and 30% in the vertical emittance, indicating that a reduction in the design emittance may be necessary. Further work should be carried out, with emphasis on mitigating the impact of synchrotron radiation at higher energy, such that a reasonable solution with a compact FFS can be found.

REFERENCES

- [1] A. Caldwell, J. Farmer, N. Lopes, A. Pukhov, F. Willeke, and T. Wilson, “Proton-driven plasma wakefield acceleration for future HEP colliders”, arXiv:2503.21669, 2025. doi:10.48550/arXiv.2503.21669
- [2] B. Foster, R. D’Arcy, and C. A. Lindström, “A hybrid, asymmetric, linear Higgs factory based on plasma-wakefield and radio-frequency acceleration”, *New J. Phys.*, vol. 25, no. 9, p. 093037, 2023. doi:10.1088/1367-2630/acf395
- [3] E. Adli *et al.*, “HALHF: a hybrid, asymmetric, linear Higgs factory using plasma- and RF-based acceleration”, arXiv:2503.19880, 2025. doi:10.48550/arXiv.2503.19880
- [4] P. Raimondi and A. Seryi, “Novel final focus design for future linear colliders”, *Phys. Rev. Lett.*, vol. 86, no. 17, pp. 3779–3782, 2001. doi:10.1103/PhysRevLett.86.3779
- [5] E. Adli *et al.*, “CLIC readiness report”, *Eur. Phys. J. Spec. Top.*, vol. 234, no. 22, pp. 6473–6652, 2026. doi:10.1140/epjs/s11734-025-02016-w
- [6] R. Brinkmann, “Optimization of a final focus system for large momentum bandwidth”, DESY, Hamburg, Germany, Rep. DESY-M-90-14, 1990.
- [7] D. Pellegrini, A. Latina, and D. Schulte, “PLACET2: A Novel Code for Beam Dynamics in Recirculating Machines”, in *Proc. IPAC’15*, Richmond, VA, USA, May 2015, pp. 465–467. doi:10.18429/JACoW-IPAC2015-MOPJE068

- [8] A. Latina, Y. Levinsen, D. Schulte, and J. Snuverink, “Evolution of the tracking code PLACET”, CERN, Geneva, Switzerland, Rep. CERN-ACC-2013-028, 2013.
- [9] D. Schulte, “Study of electromagnetic and hadronic background in the interaction region of the TESLA collider”, Ph.D. thesis, University of Hamburg, Hamburg, Germany, 1997.
- [10] H. Grote and F. Schmidt, “MAD-X: An upgrade from MAD8”, CERN, Geneva, Switzerland, Rep. CERN-AB-2003-024-ABP, 2003.
- [11] O. R. Blanco, R. Tomás, and P. Bambade, “2D-Oide effect”, CERN, Geneva, Switzerland, Rep. CERN-ACC-2015-0130, 2015.
- [12] R. Tomás, “MAPCLASS: a code to optimize high order aberrations”, CERN, Geneva, Switzerland, Rep. CERN-AB-Note-2006-017, 2006.
- [13] D. Martinez, A. Rosam, R. Tomás, and R. De Maria, “MAPCLASS2: a code to aid the optimisation of lattice design”, CERN, Geneva, Switzerland, Rep. CERN-ATS-2012-252, 2012.
- [14] R. Tomás, “Nonlinear optimization of beam lines”, *Phys. Rev. ST Accel. Beams*, vol. 9, no. 8, p. 081001, 2006.
[doi:10.1103/PhysRevSTAB.9.081001](https://doi.org/10.1103/PhysRevSTAB.9.081001)

PREPRINT